Eur Biophys J (1987) 15: 35–45

European Biophysics Journal

A new approach to polarized fluorescence using phase and modulation fluorometry

I. Theory with reference to hindered and anisotropic rotations

B. W. Van der Meer[1]*, H. Pottel[2], and W. Herreman[2]

[1] Dept. of Pharmacology, University of Texas, Health Science Center at Dallas, 5323 Harry Hines Boulevard, Dallas, Texas 75235, USA
[2] Interdisciplinair Research Centrum, Katholieke Universiteit Leuven, Campus Kortrijk, B-8500 Kortrijk, Belgium

Received April 1, 1986/ Accepted in revised form January 3, 1987

Abstract. The usual method to obtain fluorescence anisotropy decay parameters from frequency domain measurements is to determine the phase angle difference between the perpendicular and parallel components of the polarized emission and the ratio of their modulated amplitudes ("differential method"). Here, an alternative method is introduced analogous to a time-resolved study of the fluorescence anisotropy ("Sine-Cosine Transform method"), in which the intensity difference is studied in the frequency domain. It is shown that the differential method is better at low steady-state fluorescence anisotropy, while the Sine-Cosine Transform method is preferable at high anisotropy values and even more preferable, if the probe rotation is strongly anisotropic or hindered, giving rise to multiple rotational diffusion phenomena.

Key words: Fluorescence anisotropy, phase fluorometry

Introduction

Phase fluorometry studies of polarized fluorescence can be used to determine rotational characteristics of molecules in isotropic solvents and lipid membranes (Weber 1978). Mantulin and Weber (1977) have shown that the in-plane and out-of-plane rotational rates for perylene in propylene glycol are different. Lakowicz and Prendergast (1978) have provided evidence for a hindrance of the diphenylhexatriene rotation in lipid bilayers. In both studies differential phase fluorometry was used at two modulation frequencies, 10 and 30 MHz.

Recently, the potential of the technique has increased enormously, since continuously variable frequency phase and modulation fluorometers have become available (Gratton and Limkeman 1983; Jameson et al. 1984). Gratton and coworkers have shown that this advanced instrumentation permits measurements with high precision of rotational correlation times in the nanosecond time range and that it is feasible to distinguish between sophisticated rotator models with one or more exponential terms (Lakowicz et al. 1985). They employed an extension of a method introduced by Weber (1977), in which they measured not only the phase-angle difference between the perpendicular and parallel polarized components of the modulated emission, but also the corresponding modulation ratio (Lakowicz et al. 1985). In the present paper we will call this approach "the differential method". Here, we introduce an alternative method in which the phase and modulation of the parallel and perpendicular components of the modulated emission are measured. From these phases and modulations the sine and cosine transform of the intensity-difference is constructed. This analysis is analogous to studying time-resolved fluorescence anisotropy in the time domain using excitation with short flashes, because there the intensity difference between the parallel and perpendicular components is studied as well (Wahl 1969). We will call our approach the "Sine-Cosine Transform method".

It is the purpose of this paper to outline the theory of polarized phase modulation fluorescence, to introduce our "Sine-Cosine Transform method" for studying rotation and orientation and to compare it with the "differential method".

Principles of polarized phase-modulation fluorescence

The exciting light is modulated sinusoidally at high frequencies, typically in the megahertz range. The

* Present address: OMRF, Thrombosis/Hematology Research Program, 825 NE 13th Street, Oklahoma City, OK 73104, USA
Offprint requests should be sent to Dr. H. Pottel

fluorescence will then also be modulated sinusoidally at the same frequency, but will be delayed by a phase-angle, Φ, due to the finite persistance of the excited state. Additionally, the modulation of the fluorescence M will be less than that of the exciting light. The parallel and perpendicular components of the modulated emission, $I_{\parallel}$ and $I_{\perp}$, have phase-angles $\Phi_{\parallel}$ and $\Phi_{\perp}$ and modulations $m_{\parallel}$ and $m_{\perp}$ respectively. A pictorial representation of the various phase-angles and demodulation factors can be conveniently given in the case of an optimal modulation, where the intensity of the exciting light $E(t)$ is proportional to

$$E(\omega t) \sim 1 + \sin \omega t\,, \tag{1}$$

where ω equals 2π times the modulation frequency and t denotes the time. Figure 1 shows the excitation (E) and the parallel ($\parallel$) and perpendicular ($\perp$) components of the modulated emission as a function of time, also the total intensity (T), $I_T = I_{\parallel} + 2I_{\perp}$ with Φ_T and m_T and the intensity difference (D) $I_D = I_{\parallel} - I_{\perp}$ with Φ_D and m_D are shown.

Note that the phase of the difference Φ_D is not equal to the phase-angle difference, Δ. Figure 1 also serves to define the "differential method" and the "Sine-Cosine Transform method". In the differential method $\Delta = \Phi_{\perp} - \Phi_{\parallel}$ and $m_{\parallel}/m_{\perp}$ is measured after measuring Φ_T and m_T, which are necessary for information on lifetimes. In the Sine-Cosine Transform method Φ_D and m_D and also Φ_T and m_T are calculated from the measured $\Phi_{\parallel}$, $\Phi_{\perp}$, $m_{\parallel}$, $m_{\perp}$ and the steady-state fluorescence anisotropy, r_s.

For a further explanation of the two approaches we refer to Fig. 2 and Table 1. Here the 4 successive

Table 1

Method	Sample measurement	Reference measurement	Sample measurement	Reference measurement
D (differential)	Cuvette contains fluorescent sample $\alpha = 54.7°$ phase $= \Phi_T + \Phi$ mod. $= m_T M$	Cuvette contains scatterer* $\alpha = 54.7°$ phase $= \Phi$ mod. $= M$	Cuvette contains fluorescent sample $\alpha = 90°$ phase** $= \Phi_{\perp} + \Phi'$ mod.** $= m_{\perp} M'$	Cuvette contains fluorescent sample $\alpha = 0°$ phase $= \Phi_{\parallel} + \Phi'$ mod. $= m_{\parallel} M'$
A (Sine-Cosine Transform)	Cuvette contains fluorescent sample $\alpha = 0°$ phase $= \Phi_{\parallel} + \Phi$ mod. $= m_{\parallel} M$	Cuvette contains scatterer* $\alpha = 0°$ phase $= \Phi$ mod. $= M$	Cuvette contains fluorescent sample $\alpha = 90°$ phase** $= \Phi_{\perp} + \Phi'$ mod.** $= m_{\perp} M'$	Cuvette contains scatterer* $\alpha = 90°$ phase $= \Phi'$ mod. $= M'$

* Scatterer = fluorescence-free solution of glycogen in distilled water

** In principle Φ' should be equal to Φ and M' should equal M; in practice, however, these parameters may change due to different instrument settings

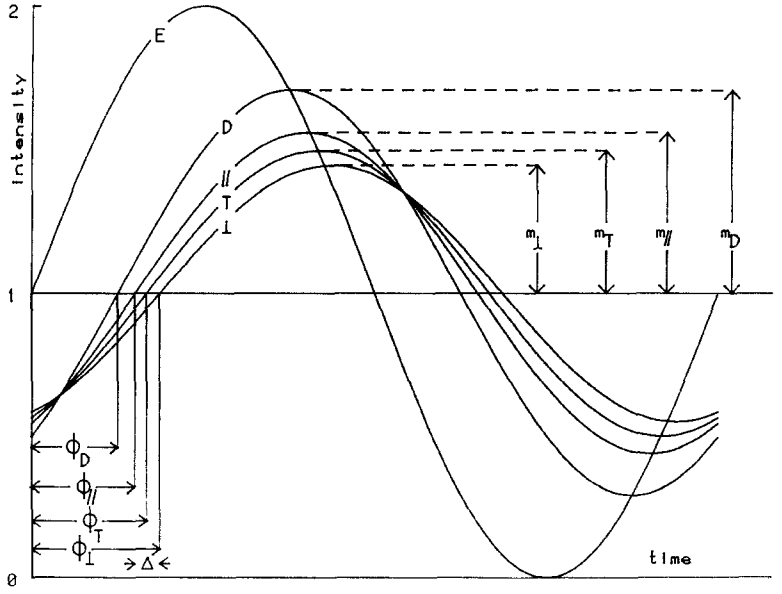

Fig. 1. Schematic diagram of the excitation (E), intensity difference (D), parallel component ($\parallel$) of the total intensity (T) and perpendicular ($\perp$) in the case of optimal modulation. The fluorescence intensities are rescaled so that

$I_D = 1 + m_D \sin(\omega t - \Phi_D)$,

$I_{\parallel} = 1 + m_{\parallel} \sin(\omega t - \Phi_{\parallel})$,

$I_T = 1 + m_T \sin(\omega t - \Phi_T)$ and

$I_{\perp} = 1 + m_{\perp} \sin(\omega t - \Phi_{\perp})$.

The phases $\Phi_{\parallel}$, $\Phi_{\perp}$, Φ_D, Φ_T are indicated together with the phase difference $\Delta = \Phi_{\perp} - \Phi_{\parallel}$; and the demodulation factors m_D, $m_{\parallel}$, m_T and $m_{\perp}$

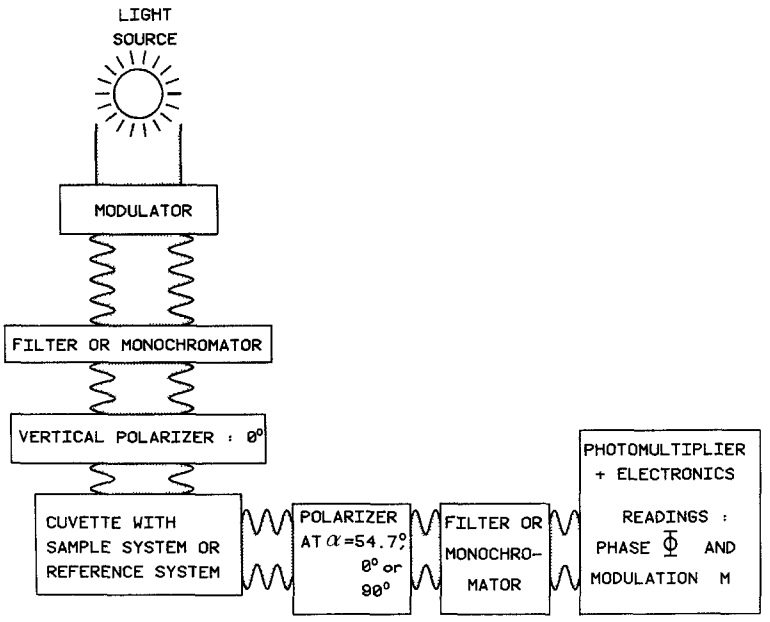

Fig. 2. Schematic diagram for the *L*-format phase modulation fluorometer

measurements necessary in both methods are shown for a *L*-format fluorometer. The case of a *T*-format fluorometer is analogous; in the latter the so-called sample and reference measurement can be combined in one measurement, so that one gets rid of the "instrumental" phases and modulation factors (see Table 1). The rotational rates and orientational order parameters to be obtained from dynamic polarization measurements cannot be evaluated without determining the lifetime (s) of the excited state. For this purpose, in the differential method one first takes a measurement with the polarizer in the emission set at the magic angle ($\alpha = 54.7°$, see Fig. 2) with respect to the vertical, so that the emission is proportional to the total intensity $I_T = I_\parallel + 2I_\perp$. In this setting one reads the phase-angle Φ_T plus an instrumental constant, Φ, and the modulation, m_T, times an instrument-dependent factor, M. Alternatively, one could obtain the same results by removing the polarizer at the emission and by setting the polarizer at the excitation at 35.3° with respect to the vertical.

This "instrumental phase", Φ, and "instrumental modulation", M, are determined in the first reference measurement, in which the fluorescent sample is replaced by a scatterer. Next, in the differential method, using an *L*-format fluorometer, the phase-difference $\Delta = \Phi_\perp - \Phi_\parallel$ and the modulation ratio $m_\parallel / m_\perp$ are obtained in two steps: First, the emission polarizer is set horizontal, i.e. perpendicular to the excitation polarizer ($\alpha = 90°$) and the phase-angle $\Phi_\perp + \Phi'$ and the modulation $m_\perp M'$ are determined; second, one measures $\Phi_\parallel + \Phi'$ and $m_\parallel M'$ with the emission polarizer in the vertical, i.e. parallel, orientation, so that the instrumental Φ' and M' are eliminated, in the difference and ratio of these values respectively. Using the *T*-format fluorometer, the phase-angle difference is obtained when one emission polarizer is rotated 90° from the parallel to the perpendicular orientation. This phase difference is always measured relative to the second photomultiplier, which always observes the phase of the perpendicular emission. At the same time, the modulation ratio can be obtained.

In the Sine-Cosine Transform method a measurement of the phase and modulation is taken with the emission polarizer set at $\alpha = 0°$ with respect to the vertical. Thus one obtains $\Phi_\parallel + \Phi$ and $m_\parallel M$. The instrumental phase Φ and modulation M are determined in the first reference measurement where the fluorescent sample is replaced by a fluorescence free scatterer. Next, $\Phi_\perp + \Phi'$ and $m_\perp M'$ are obtained from a measurement with $\alpha = 90°$. Finally, Φ' and M' are measured, again with a scattering solution in the cuvette. The phase Φ' and modulation M' should not depend on α. In practice, however, it may be necessary to change the instrumental settings, so that Φ' may differ from Φ and M' may no longer be equal to M. Thus, one measures $\Phi_\parallel$, $\Phi_\perp$, $m_\parallel$ and $m_\perp$. From these values one can calculate Φ_T and m_T, containing information on the lifetimes, and Φ_D and m_D, from which the orientation and rotations of the fluorophore can be derived. In this calculation r_s, the steady-state fluorescence anisotropy, is needed as well and can be measured in the same instrument with the modulation turned off ($\omega = 0$). The equations translating $\Phi_\parallel$, $m_\parallel$, $\Phi_\perp$ and $m_\perp$ into Φ_T, m_T, Φ_D and m_D are given in the next section.

Theory

Consider two cuvettes, one containing fluorescent molecules and the other containing a fluorescence-free scattering solution. Both are illuminated simultaneously by light modulated sinusoidally at circular frequency, ω. The scattered intensity reflects the exciting light, is similarly modulated and can be described as being proportional to

$$E(\omega t) \sim 1 + M_R \sin \omega t\,, \tag{2}$$

where M_R is the modulation of the scattered (or exciting) light and t denotes the time. Equation (1) is a special case of Eq. (2): in the former the modulation was considered complete: $M_R = 1$. In practice M_R is smaller than unity. The modulated excitation can be considered as a series of successive short flashes. The fluorescence (from the other cuvette) at time t can be calculated by summing all the responses to those flashes preceding it. If $I(t)$ is the fluorescence response to a short exciting flash, the fluorescence response to sinusoidally modulated excitation is then proportional to

$$\begin{aligned} F(\omega t) &\sim \\ &\sim \int_{-\infty}^{t} I(t-t')\,(1 + M_R \sin \omega t')\,\mathrm{d}t' \Big/ \int_{-\infty}^{t} I(t-t')\,\mathrm{d}t' \\ &\sim \int_{0}^{\infty} I(x)\,[1 + M_R \sin \omega (t-x)]\,\mathrm{d}x \Big/ \int_{0}^{\infty} I(x)\,\mathrm{d}x \\ &\sim 1 + M_R\, G \sin \omega t - M_R\, S \cos \omega t\,, \end{aligned} \tag{3}$$

where the integration variable has been changed from t' to $x = t - t'$, the lower and upper integration boundaries have been interchanged in the second line, $\sin \omega (t-x)$ is replaced by $\sin \omega t \cos \omega x - \cos \omega t \sin \omega x$, and G and S are introduced in the third line. G and S are defined as the sine and cosine transforms of $I(t)$,

$$G = \int_{0}^{\infty} I(t) \cos \omega t\,\mathrm{d}t \Big/ \int_{0}^{\infty} I(t)\,\mathrm{d}t \tag{4a}$$

$$S = \int_{0}^{\infty} I(t) \sin \omega t\,\mathrm{d}t \Big/ \int_{0}^{\infty} I(t)\,\mathrm{d}t\,. \tag{4b}$$

Equation (3) can be rewritten as

$$F(\omega t) \sim 1 + m\, M_R \sin (\omega t - \Phi) \tag{5}$$

where the phase Φ and modulation m of $F(\omega t)$ are defined according to

$$\Phi = \tan^{-1}(S/G) \tag{6a}$$

$$m = (S^2 + G^2)^{1/2}\,. \tag{6b}$$

So that

$$G = m \cos \Phi \tag{7a}$$

$$S = m \sin \Phi\,. \tag{7b}$$

The parallel ($\parallel$) and perpendicular ($\perp$) components of the emission response to a short excitation flash are related to the total fluorescence intensity, $I_T(t)$, and the fluorescence anisotropy, $r(t)$, according to:

$$I_\parallel(t) = \tfrac{1}{3} I_T(t)\,[1 + 2r(t)] \tag{8a}$$

$$I_\perp(t) = \tfrac{1}{3} I_T(t)\,[1 - r(t)]\,. \tag{8b}$$

The transforms $G_\parallel$, $S_\parallel$, $G_\perp$, $S_\perp$, G_T and S_T can be calculated following the rules of Eq. (4) from $I_\parallel(t)$, $I_\perp(t)$ and $I_T(t)$ respectively. From these transforms $\Phi_\parallel$, $m_\parallel$, $\Phi_\perp$, $m_\perp$, Φ_T and m_T are derived using Eq. (6).

Similarly, one defines

$$G_D = \int_{0}^{\infty} [I_\parallel(t) - I_\perp(t)] \cos \omega t\,\mathrm{d}t \Big/ \int_{0}^{\infty} [I_\parallel(t) - I_\perp(t)]\,\mathrm{d}t \tag{9a}$$

$$S_D = \int_{0}^{\infty} [I_\parallel(t) - I_\perp(t)] \sin \omega t\,\mathrm{d}t \Big/ \int_{0}^{\infty} [I_\parallel(t) - I_\perp(t)]\,\mathrm{d}t\,. \tag{9b}$$

G_D is the cosine transform and S_D the sine transform of the intensity difference $I_\parallel(t) - I_\perp(t)$.

G_D and S_D can be calculated from $\Phi_\parallel$, $\Phi_\perp$, $m_\parallel$, $m_\perp$ and r_s, the steady-state fluorescence anisotropy:

$$G_D = [\tfrac{1}{3}(1 + 2r_s)\, m_\parallel \cos \Phi_\parallel - \tfrac{1}{3}(1 - r_s)\, m_\perp \cos \Phi_\perp]/r_s \tag{10a}$$

$$S_D = [\tfrac{1}{3}(1 + 2r_s)\, m_\parallel \sin \Phi_\parallel - \tfrac{1}{3}(1 - r_s)\, m_\perp \sin \Phi_\perp]/r_s\,. \tag{10b}$$

These equations follow from Eq. (9) by

1. Elimination of the integrals $\int_0^\infty I_k \,\mathrm{trg}\, \omega t\,\mathrm{d}t$ ($I_k = I_\parallel$ or $I_\perp$, trg = sin or cos) using the definitions $G_\parallel = m_\parallel \cos \Phi_\parallel$, $G_\perp = m_\perp \cos \Phi_\perp$, $S_\parallel = m_\parallel \sin \Phi_\parallel$ and $S_\perp = m_\perp \sin \Phi_\perp$ analogous to Eq. (4).

2. Substitution of

$$\int_{0}^{\infty} I_\parallel(t)\,\mathrm{d}t \Big/ \int_{0}^{\infty} I_T(t)\,\mathrm{d}t = \tfrac{1}{3}(1 + 2r_s)$$

and

$$\int_{0}^{\infty} I_\perp(t)\,\mathrm{d}t \Big/ \int_{0}^{\infty} I_T(t)\,\mathrm{d}t = \tfrac{1}{3}(1 - r_s)\,.$$

Analogously one calculates

$$G_T = \tfrac{1}{3}(1 + 2r_s)\, m_\parallel \cos \Phi_\parallel + \tfrac{2}{3}(1 - r_s)\, m_\perp \cos \Phi_\perp \tag{11a}$$

$$S_T = \tfrac{1}{3}(1 + 2r_s)\, m_\parallel \sin \Phi_\parallel + \tfrac{2}{3}(1 - r_s)\, m_\perp \sin \Phi_\perp\,. \tag{11b}$$

Equations (10) and (11) are very important in the transform method. In the differential method $\Phi_T = \tan^{-1}(S_T/G_T)$ and $m_T = (S_T^2 + G_T^2)^{1/2}$ are measured directly by setting the polarizer in the emission at the magic angle with respect to the vertical (Fig. 2 and Table 1). In this way the emission is proportional to the total intensity, I_T. Instead of G_D and S_D one measures in the differential approach

$$\tan \Delta = \frac{\tan \Phi_\perp - \tan \Phi_\parallel}{1 + \tan \Phi_\perp \tan \Phi_\parallel} = \frac{S_\perp G_\parallel - S_\parallel G_\perp}{G_\parallel G_\perp - S_\parallel S_\perp} \tag{12}$$

and the modulation ratio $m_\parallel/m_\perp$ (Weber 1978; Lakowicz et al. 1985). Lakowicz et al. use unnormalized expressions for the sine and cosine transforms and, consequently, their modulation ratio Γ differs from $m_\parallel/m_\perp$:

$$\Gamma = \frac{1 + 2r_s}{1 - r_s} \frac{m_\parallel}{m_\perp} = \frac{1 + 2r_s}{1 - r_s} \left[\frac{S_\parallel^2 + G_\parallel^2}{S_\perp^2 + G_\perp^2} \right]^{1/2} . \tag{13}$$

In order to evaluate rotational and orientational order parameters from dynamic depolarization measurements in the frequency domain, a model for the fluorescence decay and the anisotropy decay must be used. A model of particular interest is the hindered rotator model in combination with a single exponential fluorescence decay. The fluorescence decay with a single lifetime τ, in response to a very short exciting flash of unit intensity is given by

$$I_T(t) = (\Phi/\tau) \exp(-t/\tau) , \tag{14}$$

where Φ is the quantum yield of emission and t is the time after excitation. In the hindered rotator model, the fluorescence anisotropy following a very short exciting pulse at time $t = 0$, may be expressed as

$$r(t) = (r_0 - r_\infty) \exp(-6Rt) + r_\infty , \tag{15}$$

where r_0 is the fundamental anisotropy in the absence of rotational diffusion and r_∞ denotes the limiting anisotropy reached at times much longer than the apparent rotational correlation time $(6R)^{-1}$; R is the apparent rotational diffusion rate (Weber 1977).

The relevant cosine and sine transforms can be readily calculated from Eqs. (4), (8), (9), (14) and (15) by applying the integrals

$$\int_0^\infty \exp(-t/\sigma) \cos \omega t \, dt = \frac{\sigma}{1 + \omega^2 \sigma^2} \tag{16a}$$

$$\int_0^\infty \exp(-t/\sigma) \sin \omega t \, dt = \frac{\omega \sigma^2}{1 + \omega^2 \sigma^2} . \tag{16b}$$

The results for the combination of models in Eqs. (14) and (15) are:

$$G_T = \frac{1}{1 + \omega^2 \tau^2} \tag{17a}$$

$$S_T = \frac{\omega \tau}{1 + \omega^2 \tau^2} \tag{17b}$$

$$G_D = \left[\frac{r_\infty}{1 + \omega^2 \tau^2} + \frac{(r_0 - r_\infty)^2 (r_s - r_\infty)}{(r_0 - r_\infty)^2 + \omega^2 \tau^2 (r_s - r_\infty)^2} \right] / r_s \tag{18a}$$

$$S_D = \omega \tau \left[\frac{r_\infty}{1 + \omega^2 \tau^2} + \frac{(r_0 - r_\infty)(r_s - r_\infty)^2}{(r_0 - r_\infty)^2 + \omega^2 \tau^2 (r_s - r_\infty)^2} \right] / r_s , \tag{18b}$$

where we have eliminated the factor $1 + 6R\tau$, appearing in (18), using the expression for the steady-state anisotropy r_s, leading to:

$$1 + 6R\tau = \frac{r_0 - r_\infty}{r_s - r_\infty} . \tag{19}$$

The corresponding formulas for $\tan \Delta$ and $m_\parallel/m_\perp$ (or Γ) have been derived by Weber (1978) and Lakowicz et al. (1985).

We will focus our attention on the combination of models for $I_T(t)$ and $r(t)$ given in Eqs. (14) and (15), because it is both simple and sufficiently general to compare the transform and differential methods. The decay behavior described by Eqs. (14) and (15) finds wide application in analyzing fluorophore dynamics in lipid membranes (Lakowicz and Prendergast 1978). Moreover, it should be noted that Eq. (15) also approximates a model for anisotropic rotation, in which $r(t)$ has a slow and a fast decaying component (Chong et al. 1985). The equations for a more general multi-exponential decay are presented in the appendix.

Comparison of the two methods

In order to compare the two methods, we introduce: $G_D^* = r_s G_D$ and $S_D^* = r_s S_D$.

The reason for this change is that the initial value (at $\omega = 0$) of G_D always equals unity, while the value of G_D^* at $\omega = 0$ becomes r_s-dependent. This makes G_D^* more sensitive to changes in system-parameters such as temperature, pH etc. Analogously, the sine transform S_D^* becomes more sensitive than S_D. For instance, in the isotropic case, the value of S_D and G_D at ω_{max} $(= r_0/(r_s \tau)$, the circular frequency where S_D or S_D^* reaches its maximal value) is always 0.5 while S_D^* and G_D^* are again r_s-dependent at ω_{max}.

It is of interest to study simulations of G_D^* and S_D^* (the transform method) in comparison with $\tan \Delta$ and Γ (the differential method) as a function

Table 2. Definitions of properties of S_D^* and G_D^* (Sine-Cosine Transform method) and of $\tan\Delta$ and M (differential method)

Transform method	Differential method
V_A = maximal value of S_D^*	V_D = maximal value of $\tan\Delta$
f_A = frequency at which S_D^* exhibits a maximum	f_D = frequency at which $\tan\Delta$ exhibits a maximum
R_A = range of $G_D^* = G_D^*(0) - G_D^*(\infty)$	R_D = range of $M = M(\infty) - M(0)$
e_A = frequency at which G_D^* exhibits an inflection	e_D = frequency at which M exhibits an inflection

of the modulation frequency. S_D^* is similar to $\tan\Delta$; both are bell shaped functions of the logarithm of the frequency. Both G_D^* and the modulation ratio Γ are monotonic functions of the frequency and exhibit an inflection point at an intermediate frequency. In comparing the two methods, it is convenient to plot $M = r_s(m_\parallel/m_\perp)$ instead of Γ, because M and G_D^* have the same value at zero frequency: $M(0) = G_D^*(0) = r_s$. Useful characteristic values of S_D^*, G_D^*, $\tan\Delta$ and M are defined in Table 2.

In different cases, one method or the other may prove preferable. The preference depends upon the relative magnitudes of the characteristic values V_A with respect to V_D, f_A in comparison with f_D, R_A with respect to R_D and e_A in comparison to e_D. We consider the differential method preferable to the transform method if:

$$V_D > V_A \text{ and/or } f_D < f_A \text{ and/or}$$
$$R_D > R_A \text{ and/or } e_D < e_A . \tag{20}$$

The transform method is considered better than the differential method, if:

$$V_A > V_D \text{ and/or } f_A < f_D \text{ and/or}$$
$$R_A > R_D \text{ and/or } e_A < e_D . \tag{21}$$

These criteria should not be taken as absolute rules, since the preference of one method over the other depends also on the instrumental details. For example, if $V_D \approx V_A$, $R_D \approx R_A$, $e_D \approx e_A$ and f_A is located midway in the frequency range available, while f_D is far above the highest frequency of the instrument, it is clear that the transform method is preferable. However, if, in the same example, f_A is still smaller than f_D, but both are much lower than the highest frequency available, both methods will be equally suitable to yield the information on the rotational behavior studied. Nevertheless, the criteria introduced above may be helpful in finding general trends in the preference of one method over the other, depending on the values of the parameters measured.

The criteria have been worked out for the combination of the hindered rotator model with the mono-exponential decay model. V_A and f_A can be calculated by differentiating $S_D^* = r_s S_D$ with respect to the frequency. They must be calculated numerically, but upper and lower bounds can readily be analytically evaluated. V_D and f_D are derived similarly from the corresponding expression of $\tan\Delta$ (Eq. (6) in Weber (1978)). The value for $e_A(e_D)$ can be calculated by differentiating G_D^* (M; Lakowicz et al. (1985)) twice with respect to the frequency ($G_D^* = r_s G_D$ in Eq. (18a)). Upper and lower bounds for e_A are given below. The range of R_A is equal to that of G_D^* at zero frequency minus G_D^* at infinite frequency, while the range of R_D is equal to that of M at infinite frequency minus M at zero frequency. The expressions for f_A, f_D, V_A, V_D, e_A, e_D, R_A and R_D read:

$$\frac{1}{2\pi\tau} \leqq f_A \leqq \frac{1}{2\pi\tau}\frac{r_0 - r_\infty}{r_s - r_\infty} \tag{22}$$

$$f_D = \frac{1}{2\pi\tau}\left[\frac{(1+2r_s)(1-r_s)}{(1+2r_0)(1-r_0)}\right]^{1/2}\frac{r_0 - r_\infty}{r_s - r_\infty} \tag{23}$$

$$\tfrac{1}{2} r_\infty \leqq V_A \leqq \tfrac{1}{2} r_s \tag{24}$$

$$V_D = \tfrac{3}{2}(r_0 - r_s)\left[\frac{(1+2r_0)(1-r_0)}{(1+2r_s)(1-r_s)}\right]^{1/2} \tag{25}$$

$$\frac{1}{2\pi\tau\sqrt{3}} \leqq e_A \leqq \frac{1}{2\pi\tau\sqrt{3}}\frac{r_0 - r_\infty}{r_s - r_\infty} \tag{26}$$

$$e_D = \frac{1}{2\pi\tau\sqrt{3}}\frac{(1-r_s)(r_0 - r_\infty)}{(1-r_0)(r_s - r_\infty)} \tag{27}$$

$$R_A = r_s \tag{28}$$

$$R_D = \frac{3 r_s (r_0 - r_s)}{(1-r_0)(1+2r_s)} . \tag{29}$$

The lower bounds in the case of f_A, V_A and e_A correspond to the situation where $r_\infty \approx r_s$ and the upper bounds correspond to $r_\infty \approx 0$.

Using the expressions (22)–(29) and the criteria (20) and (21), the region formed by all possible (r_s, r_∞) combinations can be divided into subregions, where one of the methods is preferable over the other. The results are shown in Fig. 3.

The regions indicated in Fig. 3 have the following meaning:

DD: The differential method is greatly preferable to the transform method, because $\tan\Delta$ is much larger than S_D^*: $V_D > 8 V_A$, while f_A and f_D are of the same

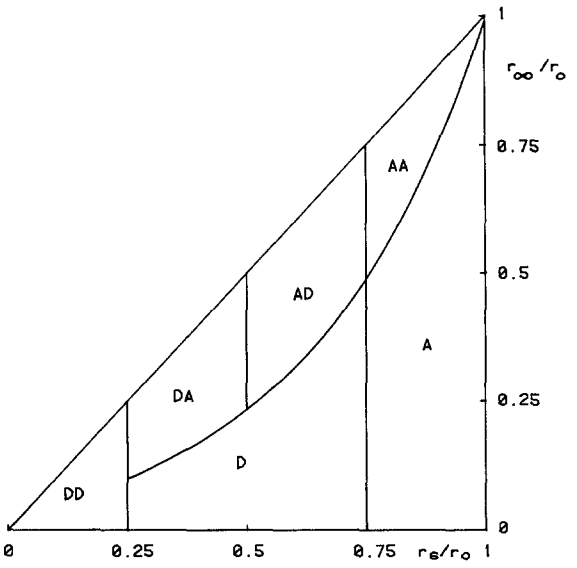

Fig. 3. Comparison of the differential method with the transform method for the hindered rotator model with monoexponential fluorescence. In region *D* the differential method is better, in *DD* it is much better, in *A* the transform method is better, while in *AA* this latter approach is strongly preferable. *DA* and *AD* refer to cases of intermediate preference (*see text*)

order of magnitude, except near $r_\infty = r_s$; R_D is larger than R_A ($1.25\,R_A < R_D < 2\,R_A$), while e_A and e_D are of the same order except near $r_\infty = r_s$.

D: The differential method is preferable, because $V_D > V_A$ ($8\,V_A > V_D > V_A$). R_D is about equal to R_A ($1.25\,R_A > R_D > 0.31\,R_A$). The frequencies are of the same order of magnitude ($f_A < f_D < 1.5\,f_A$, $e_A < e_D < 2\,e_A$).

DA: Region where the preference is arbitrary. $8\,V_A > V_D > 3\,V_A$, $f_D > 1.5\,f_A$, $1.25\,R_A > R_D > 0.71\,R_A$, $e_D > 4\,e_A$.

AD: Region where the preference is arbitrary. $V_D > V_A > 0.33\,V_D$, $f_A < 0.67 f_D$, $3.2\,R_D > R_A > 1.4\,R_D$, $e_A < 0.5\,e_D$.

A: The transform method is preferable, because both $V_A > V_D$ and $R_A > 3.2\,R_D$. The frequencies are of the same order of magnitude: $f_D > f_A > 0.67\,f_D$, $e_D > e_A > 0.5\,e_D$.

AA: The transform method is much more favorable, because both $V_A > V_D$ and $R_A > 3.2\,R_D$. Moreover, f_A is lower than f_D ($f_A < 0.67\,f_D$) and e_A is lower than e_D ($e_A < 0.5\,e_D$).

It should be noted that, in the calculation of the boundaries in Fig. 3, the approximation $r_0 = 0.4$ has been employed. For other values of r_0, especially for negative r_0 values, the boundary may deviate somewhat from the ones in Fig. 3. To illustrate the difference between the results of the two methods,

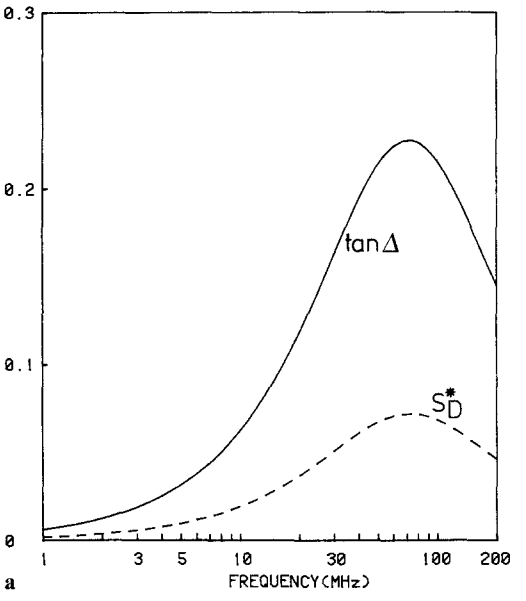

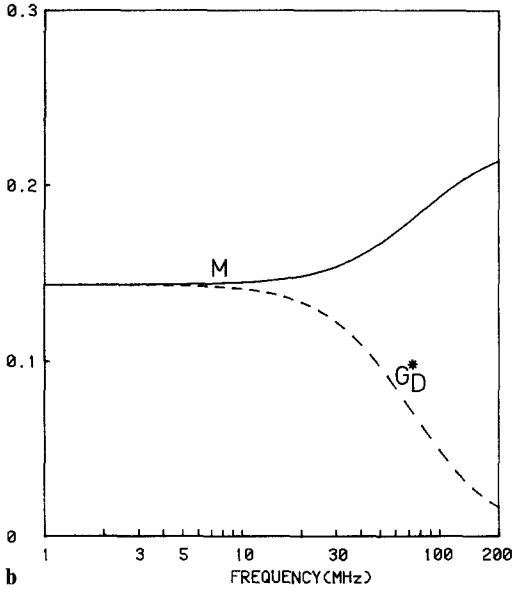

Fig. 4a,b. Simulations of S_D^*, $\tan\Delta$ (**a**), G_D^* and M (**b**) as a function of frequency for the case $r(t) = 0.312\exp(-t/4.09)$ (t in ns) and $\tau = 4.8$ ns, $r_s = 0.144$. This example belongs to region *D* in Fig. 3. The M and $\tan\Delta$ curves correspond to real data (Lakowicz et al. 1985) for perylene in propylene glycol at $-9\,^\circ$C (their Fig. 2)

simulations have been made of S_D^*, $\tan\Delta$, G_D^* and M as functions of frequency. Examples are shown in Figs. 4 and 5 (isotropic case) and Figs. 6 and 7 (hindered rotation case).

So far we have restricted our attention to the hindered rotator model. However, it should be noted that this model is very similar to an anisotropic rotator model with a slow and a fast decaying component (Chong et al. 1985). Therefore, one would expect that for anisotropic rotators, the transform method is better, if the deviation from iso-

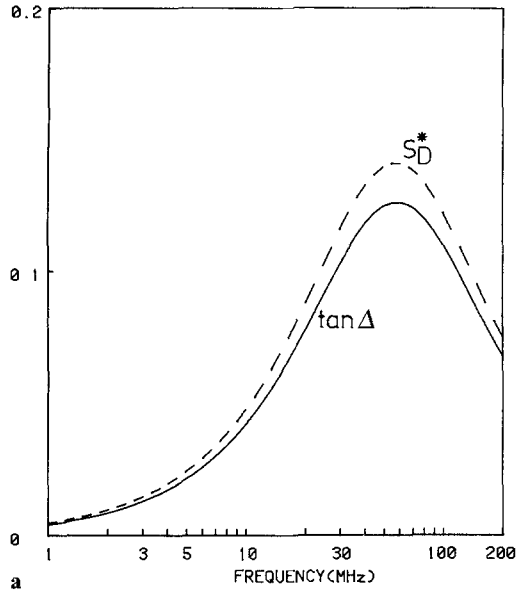

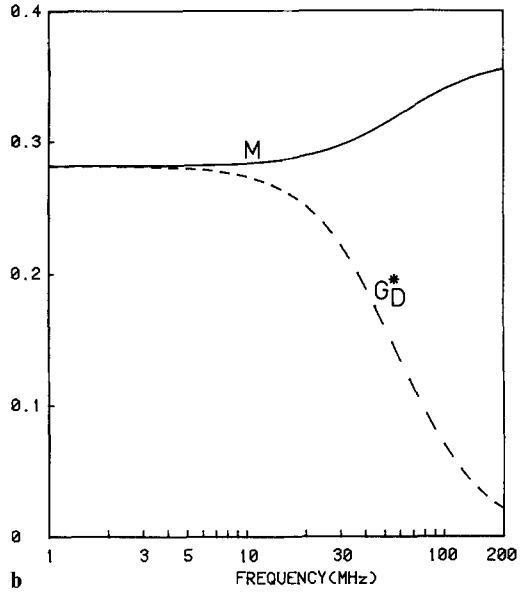

Fig. 5 a, b. Simulations of S_D^*, $\tan\Delta$ (**a**), G_D^* and M (**b**) as a function of frequency for the case $r(t) = 0.375 \exp(-t/11.2)$ (t in ns) and $\tau = 3.7$ ns, $r_s = 0.282$. This example refers to the region A in Fig. 3. The M and $\tan\Delta$ curves correspond to real data (Lakowicz et al. 1985) for fluorescein in propylene glycol at 15 °C (their Fig. 1)

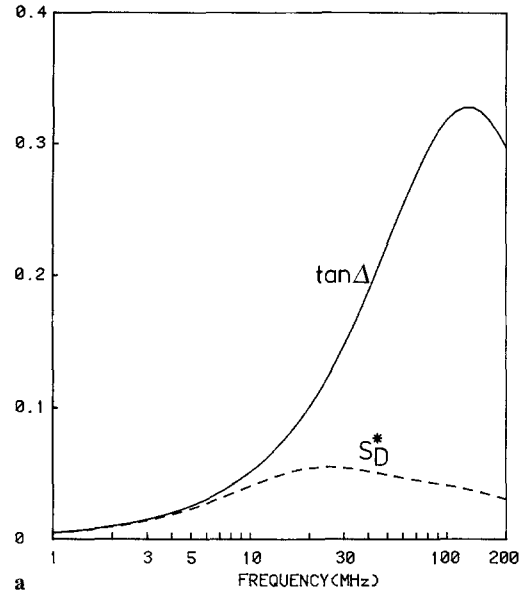

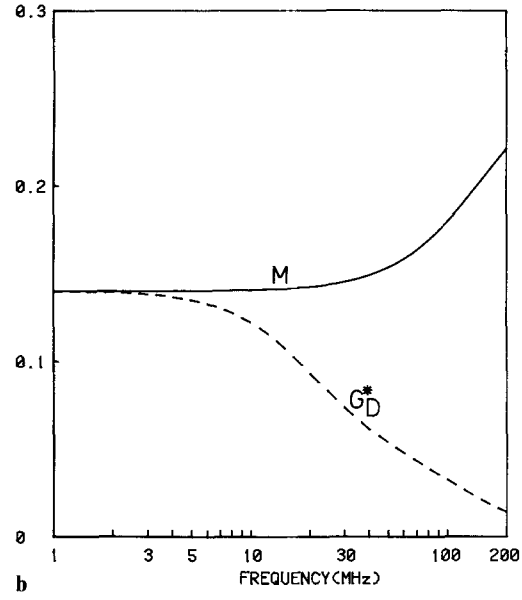

Fig. 6 a, b. Simulations of S_D^*, $\tan\Delta$ (**a**), G_D^* and M (**b**) as a function of frequency for the case $r(t) = 0.286 \exp(-t/1.5) + 0.094$ (t in ns), $\tau = 7.8$ ns, $r_s = 0.140$. This example corresponds to region DA in Fig. 3. The M and $\tan\Delta$ curves correspond to real data (Lakowicz et al. 1985) for DPH in DMPC vesicles at 39 °C (their Fig. 5)

tropic rotation behavior is pronounced and r_s/r_0 is large, whereas the differential method is expected to be preferable, in the case that the rotational rates are close to each other and r_s/r_0 is small. As an illustration of this trend, we have included a simulation of a strongly anisotropic rotator (Fig. 8). Note that $f_A \approx e_A \approx 30$ MHz, that is, much shorter and therefore more easy to detect than f_D and e_D, which are both larger than 200 MHz.

Discussion

In this paper we have introduced a new method to study free and hindered rotations using phase-modulation fluorometry. In the usual method, the differential method, the phase difference, $\Phi_\perp - \Phi_\parallel$, between the parallel and perpendicular component and their modulation ratio are measured. Our approach is more analogous to studies of the fluores-

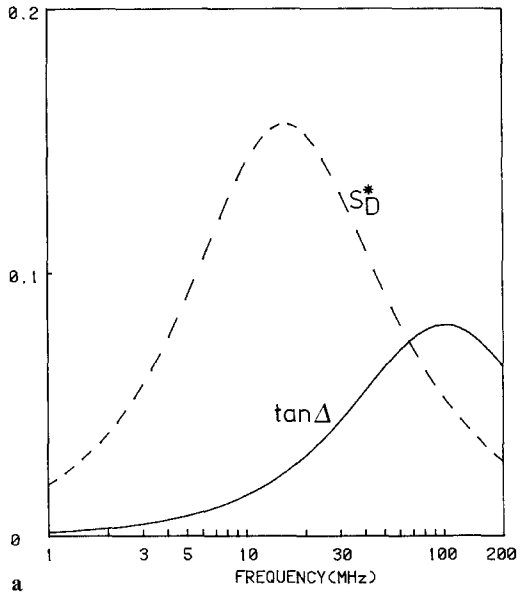

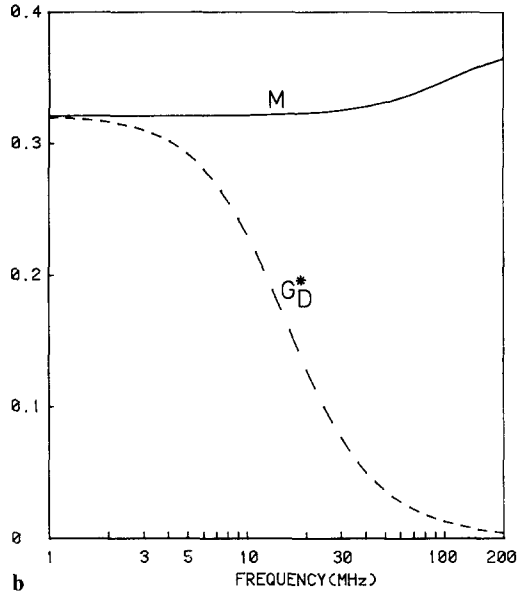

Fig. 7a,b. Simulations of S_D^*, $\tan\Delta$ (**a**), G_D^* and M (**b**) as a function of frequency for the case $r(t) = 0.07\exp(-t/1.9) + 0.31$ (t in ns), $\tau = 10.2$ ns, $r_s = 0.321$. This example corresponds to *AA* in Fig. 3. The M and $\tan\Delta$ curves correspond to real data (Lakowicz et al. 1985) for DPH in DMPC vesicles at 7 °C (their Fig. 5)

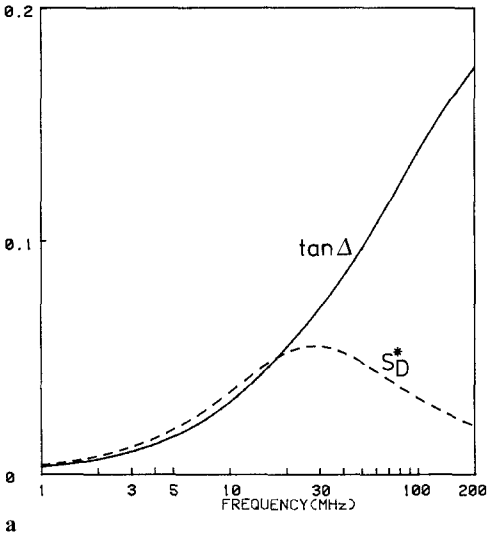

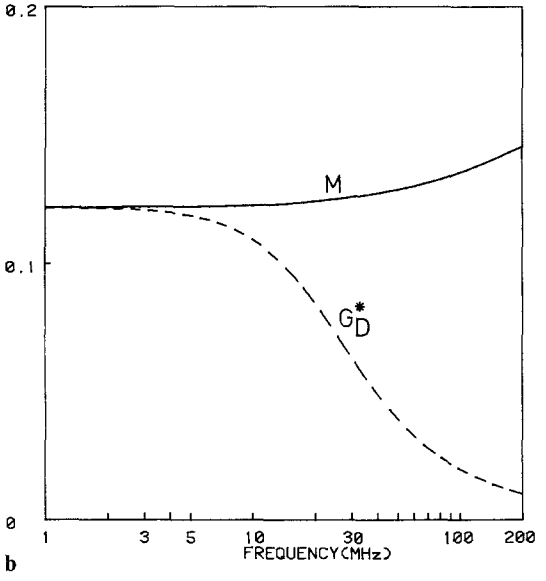

Fig. 8a,b. Simulations of S_D^*, $\tan\Delta$ (**a**), G_D^* and M (**b**) as a function of frequency for the case $r(t) = 0.158\exp(-t/0.20) + 0.072\exp(-t/1.46) + 0.120\exp(-t/46.7)$ (t in ns) and $\tau = 6.81$ ns, $r_s = 0.122$. This example is analogous to a point in the *AA* region in Fig. 3. The M and $\tan\Delta$ curves correspond to real data (Lakowicz et al. 1985) for perylene in DMPC at 5 °C (their Fig. 7)

cence anisotropy in the time domain, because in the "Sine-Cosine Transform method" the phase and modulation of the parallel and perpendicular components of the modulated emission are measured. From these phases and modulations, the sine and cosine transform of the intensity difference, $I_\parallel - I_\perp$, is constructed. The two approaches have been compared with special reference to the hindered rotator model combined with a mono-exponential fluorescence decay (equations for more general models are presented in the appendix). The conclusion is that the differential method is preferable at relatively low values of r_s, the steady-state fluorescence anisotropy, while the transform method is better at high r_s, especially if the rotational motion is strongly hindered (high r_∞) or strongly anisotropic (see Fig. 3). The trend is in agreement with Weber's finding that the unique maximal $\tan\Delta$-value that

obtains for any isotropic rotator is reduced if the rotations are anisotropic or hindered (Weber 1978).

Apart from theoretical considerations, it is also necessary to consider certain practical aspects of the different measurements. In the transform method $\Phi_\parallel$, $\Phi_\perp$, $m_\parallel$ and $m_\perp$ are measured with respect to a scattering solution. Consequently, the phototubes alternately observe light at different wavelengths. If there should be an appreciable wavelength-dependence of the time response of the phototubes, this alternating observation of fluorescent and scattered light may cause some systematic errors. In the differential method, on the other hand, the photomultiplier tubes always observe light at the same wavelength in measuring $\Phi_\perp - \Phi_\parallel$ and $m_\parallel/m_\perp$. Therefore, the measurement will in no way be affected by any such wavelength dependence of the phototube response. To overcome this drawback of the transform method, it is always possible to obtain $\Phi_\parallel$ and $\Phi_\perp$ from the measurement of the phase differences $\Phi_\parallel - \Phi_T$ and $\Phi_\perp - \Phi_T$ respectively, after the determination of Φ_T with respect to a scatterer. In this way $\Phi_\parallel$ and $\Phi_\perp$ are obtained by a differential method but the data-analysis can be carried out by the transform method. The procedure indicated has the additional advantage that the random errors in $\Phi_\parallel$ and $\Phi_\perp$ will decrease, so that the signal-to-noise ratio of the measurable parameters in the transform method is expected to become equivalent to that of the differential method. Another possible source of error is that the sensitivity of the emission detector is slightly different for parallel polarized light and perpendicular polarized light. This possible systematic error will affect the results in the differential method, but not the results in the transform method. Whether or not these possible systematic errors are of importance, is not clear as yet and must be investigated experimentally. A detailed comparison of the results of the two methods applied to a specific test system, should be helpful in evaluating such systematic errors.

Acknowledgements. The authors would like to thank Dr. David Jameson (Dallas, Texas) and Dr. Enrico Gratton (Urbana, Illinois) for helpful comments.

Appendix

In general, the total intensity $I_T(t)$ and the fluorescence anisotropy $r(t)$ after a very short flash excitation can be expressed as sums of exponentials:

$$I_T(t) = \sum_{i=1}^{N} \alpha_i \exp(-t/\tau_i) \tag{A1}$$

$$r(t) = \sum_{j=1}^{M} g_j \exp(-6R_j t)\,, \tag{A2}$$

where α_i and g_j are the pre-exponentials, with $\sum g_j = r_0$, and τ_i denote the lifetimes and R_j the rotational rates. $I_T(t)$ contains N and $r(t)$ M exponential terms.

Using Eqs. (16a), (16b), (4a) and (4b), the various sine and cosine transforms can be calculated:

$$G_T = \int_0^\infty I_T(t) \cos\omega t \, dt \Big/ \int_0^\infty I_T(t)\, dt = \sum_i \{\alpha_i \tau_i/(1+\omega^2\tau_i^2)\} \Big/ \sum_i \alpha_i \tau_i \tag{A3a}$$

$$S_T = \sum_i \{\alpha_i \omega \tau_i^2/(1+\omega^2\tau_i^2)\} \Big/ \sum_i \alpha_i \tau_i \tag{A3b}$$

$$G_D = \int_0^\infty r(t)\, I_T(t) \cos\omega t \, dt \Big/ \int_0^\infty r(t)\, I_T(t)\, dt$$
$$= \sum_i \sum_j \{\alpha_i g_j \tau_i (1+6R_j\tau_i)/((1+6R_j\tau_i)^2+\omega^2\tau_i^2)\} \Big/ \sum_i \sum_j \alpha_i g_j \tau_i (1+6R_j\tau_i)^{-1} \tag{A4a}$$

$$S_D = \sum_i \sum_j \{\alpha_i g_j \omega \tau_i^2/((1+6R_j\tau_i)^2+\omega^2\tau_i^2)\} \Big/ \sum_i \sum_j \alpha_i g_j \tau_i (1+6R_j\tau_i)^{-1} \tag{A4b}$$

$$r_s = \sum_i \sum_j \alpha_i g_j \tau_i/(1+6R_j\tau_i) \tag{A4c}$$

$$G_{\parallel} = \int_0^{\infty} (I_T(t) + 2 I_T(t)\, r(t)) \cos\omega t \, \mathrm{d}t / \int_0^{\infty} (I_T(t) + 2 I_T(t)\, r(t)) \, \mathrm{d}t$$
$$= \left\{\sum_i \alpha_i \tau_i/(1+\omega^2\tau_i^2)\right\} / \left\{\sum_i \alpha_i \tau_i + 2 \sum_i \sum_j \alpha_i g_j (1+6R_j\tau_i)^{-1}\right\}$$
$$+ 2\left\{\sum_i \sum_j \alpha_i \tau_i g_j (1+6R_j\tau_i)/((1+6R_j\tau_i)^2+\omega^2\tau_i^2)\right\} / \left\{\sum_i \alpha_i \tau_i + 2 \sum_i \sum_j \alpha_i g_j (1+6R_j\tau_i)^{-1}\right\} \quad \text{(A5a)}$$

$$S_{\parallel} = \left\{\sum_i \alpha_i \omega \tau_i^2/(1+\omega^2\tau_i^2)\right\} / \left\{\sum_i \alpha_i \tau_i + 2 \sum_i \sum_j \alpha_i g_j (1+6R_j\tau_i)^{-1}\right\}$$
$$+ 2\left\{\sum_i \sum_j \alpha_i g_j \omega \tau_i^2/((1+6R_j\tau_i)^2+\omega^2\tau_i^2)\right\} / \left\{\sum_i \alpha_i \tau_i + 2 \sum_i \sum_j \alpha_i g_j (1+6R_j\tau_i)^{-1}\right\} \quad \text{(A5b)}$$

$$G_{\perp} = \int_0^{\infty} (I_T(t) - I_T(t)\, r(t)) \cos\omega t \, \mathrm{d}t / \int_0^{\infty} (I_T(t) - I_T(t)\, r(t)) \, \mathrm{d}t$$
$$= \left\{\sum_i \alpha_i \tau_i/(1+\omega^2\tau_i^2)\right\} / \left\{\sum_i \alpha_i \tau_i - \sum_i \sum_j \alpha_i g_j (1+6R_j\tau_i)^{-1}\right\}$$
$$- \left\{\sum_i \sum_j \alpha_i g_j \tau_i (1+6R_j\tau_i)/((1+6R_j\tau_i)+\omega^2\tau_i^2)\right\} / \left\{\sum_i \alpha_i \tau_i - \sum_i \sum_j \alpha_i g_j (1+6R_j\tau_i)^{-1}\right\} \quad \text{(A6a)}$$

$$S_{\perp} = \left\{\sum_i \alpha_i \omega \tau_i^2/(1+\omega^2\tau_i^2)\right\} / \left\{\sum_i \alpha_i \tau_i - \sum_i \sum_j \alpha_i g_j (1+6R_j\tau_i)^{-1}\right\}$$
$$- \left\{\sum_i \sum_j \alpha_i g_j \omega \tau_i^2/((1+6R_j\tau_i)^2+\omega^2\tau_i^2)\right\} / \left\{\sum_i \alpha_i \tau_i - \sum_i \sum_j \alpha_i g_j (1+6R_j\tau_i)^{-1}\right\} \quad \text{(A6b)}$$

$$\tan(\Phi_{\perp} - \Phi_{\parallel}) = (S_{\perp} G_{\parallel} - S_{\parallel} G_{\perp})/(G_{\perp} G_{\parallel} - S_{\perp} S_{\parallel}) \quad \text{(A7a)}$$

$$m_{\parallel}/m_{\perp} = \{(S_{\parallel}^2 + G_{\parallel}^2)/(S_{\perp}^2 + G_{\perp}^2)\}^{1/2}. \quad \text{(A7b)}$$

References

Chong PLG, van der Meer BW, Thompson TE (1985) Rotational motions of perylene in lipid bilayers: Pressure and cholesterol effects. Biochim Biophys Acta 813:253–265

Gratton E, Limkeman M (1983) A continuously variable frequency cross-correlation phase fluorometer with picosecond resolution. Biophys J 44:315–324

Jameson DM, Gratton E, Hall RD (1984) The measurement and analysis of heterogeneous emissions by multifrequency phase and modulation fluorometry. Appl Spectrosc Rev 20:55–65

Lakowicz JR, Prendergast FG (1978) Quantitation of hindered rotations of diphenylhexatriene in lipid bilayers by differential polarized phase fluorometry. Science 200:1399–1401

Lakowicz JR, Cherek H, Maliwal BP, Gratton E (1985) Time resolved fluorescence anisotropies of diphenylhexatriene and perylene in solvents and lipid bilayers obtained from multifrequency phase-modulation fluorometry. Biochemistry 24:376–383

Mantulin WW, Weber G (1977) Rotational anisotropy and solvents fluorophore bonds: An investigation by differential polarized phase fluorometry. J Chem Phys 66:4092–4099

Wahl Ph (1969) Mesure de la décroissance de la fluorescence polarisée de la gamma globuline D.N.S. Biochim Biophys Acta 175:55–64

Weber G (1977) Theory of differential phase fluorometry. Detection of anisotropic molecular rotations. J Chem Phys 66:4081–4091

Weber G (1978) Limited rotational motion: Recognition by differential phase fluorometry. Acta Phys Pol A54: 859–865